



Small-displacement measurements using high-order Hermite-Gauss modes

Hengxin Sun, Kui Liu, Zunlong Liu, Pengliang Guo, Junxiang Zhang, and Jiangrui Gao

Citation: [Applied Physics Letters](#) **104**, 121908 (2014); doi: 10.1063/1.4869819

View online: <http://dx.doi.org/10.1063/1.4869819>

View Table of Contents: <http://scitation.aip.org/content/aip/journal/apl/104/12?ver=pdfcov>

Published by the [AIP Publishing](#)

Articles you may be interested in

[Interferometric Measurement of Displacements](#)

Phys. Teach. **45**, 405 (2007); 10.1119/1.2783143

[Displacement measurement in real time using the attenuated total reflection technique](#)

Appl. Phys. Lett. **84**, 3253 (2004); 10.1063/1.1715146

[Six-degree-of-freedom displacement measurement system using a diffraction grating](#)

Rev. Sci. Instrum. **71**, 3214 (2000); 10.1063/1.1305816

[Displacement measurement and surface profiling using semi-insulating photoconductive semiconductors and linearly frequency-ramped lasers](#)

Appl. Phys. Lett. **75**, 1374 (1999); 10.1063/1.124698

[Guidance characteristics of some displacement devices used in a high-precision He–Ne laser displacement measurement system](#)

Rev. Sci. Instrum. **68**, 2913 (1997); 10.1063/1.1148219



Re-register for Table of Content Alerts

Create a profile.



Sign up today!



Small-displacement measurements using high-order Hermite-Gauss modes

Hengxin Sun, Kui Liu, Zunlong Liu, Pengliang Guo, Junxiang Zhang, and Jiangrui Gao^{a)}
 State Key Laboratory of Quantum Optics and Quantum Optics Devices, Institute of Opto-Electronics,
 Shanxi University, Taiyuan 030006, China

(Received 10 February 2014; accepted 17 March 2014; published online 26 March 2014)

We present a scheme for small-displacement measurements using high-order Hermite-Gauss modes and balanced homodyne detection. We demonstrate its use with experimental results of displacement measurements using fundamental transverse mode TEM_{00} and first order transverse mode TEM_{10} as signal modes. The results show a factor of 1.41 improvement in measurement precision with the TEM_{10} mode compared with that with the TEM_{00} mode. This scheme has potential applications in precision metrology, atomic force microscopy, and optical imaging. © 2014 AIP Publishing LLC. [<http://dx.doi.org/10.1063/1.4869819>]

Optical displacement measurements are one of several basic techniques in the precision measurement toolbox. Even for very high precision measurements, they have been widely used in many areas such as atomic force microscopy,^{1,2} optical tweezer,^{3–5} optical imaging,^{6–8} biological measurement,⁹ and even gravitational wave detection.¹⁰ In general, measurement precision is limited ultimately by quantum noise and for that reason has become a very challenging field. Two methods have been used to improve the signal-to-noise ratio (SNR) or precision. One involves reducing the quantum noise using spatial squeezing and entanglement techniques.^{9,11–13} Treps *et al.* devised a spatial squeezed light of 3.3-dB squeezing, obtaining a factor of 1.5 precision improvement compared with the classical limit.¹¹ The other involves enhancing the detection efficiency by optimizing the detection setup. For example, homodyne detection has been proved to be better than split detection in displacement measurements.^{14,15} Parallel research on weak-value measurements has also greatly improved the SNR of beam deflection measurements.^{16,17}

In this Letter, we present and demonstrate experimentally a scheme for optical displacement measurements based on high-order Hermite-Gauss modes and balanced homodyne detection (BHD). Displacement measurements with TEM_{00} and TEM_{10} modes as signal beams are realized. A factor of 1.41 improvement is obtained in measurement precision for the TEM_{10} mode compared with that for the TEM_{00} mode. The results obtained are equivalent to that with a 3-dB spatially squeezed light system although our scheme is the more practical and more robust to losses. Indeed, some applications based on high-order Hermite-Gauss modes have been reported in some areas such as optical imaging¹⁸ and tracking of single atom.¹⁹

There are two methods often used in beam displacement measurements: the split detection and balanced homodyne detection. The split detection is only 80% efficient compared with TEM_{10} homodyne detection with a TEM_{00} signal beam.¹⁴ Hence we shall only concentrate on the latter in this Letter.

Any small transverse displacement d of a $TEM_{n,0}$ mode $u_n(x)$ leads to an excitation of the other order mode. Here, n denotes the order of the x -axis Hermite-Gauss mode. Using a Taylor series expansion, we have

$$u_n(x+d) = u_n(x) + u'_n(x)d + \sum_{m \geq 2} \frac{u_n^{(m)}(x)}{m!} d^m, \quad (1)$$

where $u'_n(x) = (\sqrt{2}/w_0) [\sqrt{n/2}u_{n-1}(x) - \sqrt{n+1/2}u_{n+1}(x)]$ is the first derivative of $u_n(x)$ with respect to x and w_0 denotes the beam waist of the TEM_{00} mode. The excited modes are mostly the neighboring order modes for $(n+1)$ and $(n-1)$,²⁰ which are included the main displacement signal. It can be measured perfectly by BHD with the matched local-oscillator mode, which has normalized expression

$$u_n^{LO}(x) = \sqrt{2/(2n+1)} [\sqrt{n/2}u_{n-1}(x) - \sqrt{n+1/2}u_{n+1}(x)]. \quad (2)$$

After the BHD system, we obtain

$$\hat{x}_s^{BHD} = \sqrt{N_{Lo}} \left(2\sqrt{2n+1}\sqrt{Nd}/w_0 + \delta\hat{X}_s^+ \right), \quad (3)$$

where N and N_{Lo} are, respectively, the signal and local-field mean photon number, $\delta\hat{X}_s^+$ is the quantum noise of the signal field, and d is the displacement. In Eq. (3), the first term represents the signal, and the second represents noise. For coherent light ($\delta^2\hat{X}_s^+ = 1$), the SNR is defined as $SNR^{BHD} = (2\sqrt{2n+1}\sqrt{Nd})^2/w_0^2$. The minimum measurable displacement is, in general, defined as the displacement with $SNR = 1$; for the BHD measurement, it is given by

$$d_{\min}^{BHD} = \frac{w_0}{2\sqrt{2n+1}\sqrt{N}}. \quad (4)$$

Clearly, the higher the mode order is, the smaller the minimum measurable displacement is, and therefore the higher the measurement precision is. This will be important in displacement measurements, especially when the optical power density should not be too intense. Damage, for example, can occur to biological specimens if beams are too intense.^{9,21}

^{a)} Author to whom correspondence should be addressed. Electronic mail: jrgao@sxu.edu.cn

Indeed, the minimum measurable information of any parameter θ of an optical beam is ultimately constrained by the quantum Cramér-Rao (QCR) bound²²

$$\delta\theta \geq \delta\theta_{\min} = \frac{\sigma_{\min}}{\sqrt{QN_{\theta}}} \left[4\|u'_{\theta=0}\|^2 + \left(\frac{N'_{\theta}}{N_{\theta}}\right) \right]^{-1/2}, \quad (5)$$

where $\delta\theta_{\min}$ is the error limit in the estimation $\hat{\theta}$, $u'_{\theta=0}$ is the derivative of the normalized transverse field distribution u_{θ} with respect to θ at $\theta=0$, N_{θ} is the mean photon number for single measurement, N'_{θ} is its derivative with respect to θ , Q is the number of measurement repetitions, and σ_{\min} is quantum noise.

For displacement measurements using a high-order $TEM_{n,0}$ signal beam, θ is replaced by the displacement d , $u'_{\theta} = \partial[u_n(x+d)]/\partial d|_{d=0}$, $N'_{\theta} = 0$, $\sigma_{\min} = 1$ as the coherent light is used, and $\|\partial[u_n(x+d)]/\partial d|_{d=0}\|^2 = (2n+1)/w_0^2$. We then obtain the QCR bound for the displacement measurement of

$$d_{\min}^{QCR} = \frac{w_0}{2\sqrt{2n+1}\sqrt{N}}. \quad (6)$$

We can see from Eqs. (4) and (6) that the BHD scheme has reached the QCR bound limit. However, generating the local mode described in Eq. (2) in an experiment is a little complicated; hence, we preliminarily choose an intermediate mode $TEM_{n+1,0}$ for the local oscillator, i.e., $u_n^{\text{int},LO}(x) = u_{n+1}(x)$. In the corresponding experiment, the BHD output and its SNR are easy to obtain

$$\hat{n}_{-}^{\text{int},BHD} = \sqrt{N_{L_0}} \left(2\sqrt{n+1}\sqrt{Nd}/w_0 + \delta\hat{X}_s^+ \right), \quad (7)$$

$$\text{SNR}^{\text{int},BHD} = (2\sqrt{n+1}\sqrt{Nd})^2/w_0^2. \quad (8)$$

The minimum measurable displacement with just the $TEM_{n+1,0}$ local-oscillator mode is then given by

$$d_{\min}^{\text{int},BHD} = \frac{w_0}{2\sqrt{n+1}\sqrt{N}}. \quad (9)$$

Equations (4) and (9) are plotted in Fig. 1, with green star and red point, respectively. Both are normalized using $w_0/2\sqrt{N}$, which represents the minimum measurable displacement with the coherent TEM_{00} -mode signal. The

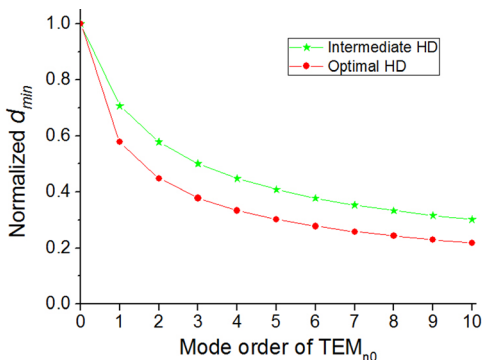


FIG. 1. Mode-order dependence of minimum measurable displacements for intermediate homodyne detection and optimal homodyne detection.

minimum measurable displacement decreases and the rate of decrease is slow as mode order increases. Furthermore, the optimal local oscillator BHD is better than the intermediate local oscillator. The difference between the two curves is relatively small, and hence the intermediate mode for the local oscillator is a good alternative in general.

A schematic of the experiment is presented in Fig. 2. A continuous wave solid-state YAG laser operating at 1064 nm is used to drive the experiment. Part of the beam is passed through mode-conversion cavity MC1, then modulated by the displacement modulation system (DMS) as the signal beam with displacement. In BHD, it is in phase with the local-oscillator mode from mode-conversion cavity MC2. The BHD output is analyzed by an electronic spectrum analyzer (ESA).

The DMS consists of a mirror mounted on a piezoelectric transducer (PZT1) and connected to a signal generator (SG). The PZT1 is driven by a sine wave signal at its mechanical resonance frequency of 3 MHz.

We generated and locked the cavity at different transverse modes by misaligning the input TEM_{00} beams into the mode-conversion cavity.^{23,24} MC1 is locked at the TEM_{00} mode (or TEM_{10} mode) to produce the signal beam, and MC2 at the TEM_{10} mode (or TEM_{20} mode) as the local-oscillator mode. With the two cavities locked to the same modes, the interference visibilities measured for the TEM_{00} , TEM_{10} , and TEM_{20} modes were 0.99 ± 0.01 , 0.98 ± 0.01 , and 0.96 ± 0.01 , respectively. The experimental parameters are: signal beam power, $P_s = 100 \mu\text{W}$; beam waist of TEM_{00} , $w_0 = 53 \mu\text{m}$; resolution bandwidth, $RBW = 30 \text{ kHz}$; video bandwidth, $VBW = 100 \text{ Hz}$; and analyzing frequency, $f = 3 \text{ MHz}$.

The measured displacement signal power vs displacement is shown in Fig. 3(a). Trace (a1) is the shot noise level (SNL) without displacement. The SNLs are the same for TEM_{10} and TEM_{20} local oscillators because the power is the same. Trace (b1) corresponds to the TEM_{00} signal mode and TEM_{10} local mode while trace (c1) to the TEM_{10} signal mode and TEM_{20} local mode. The TEM_{00} and the TEM_{10} signal-beam powers are also the same. The detector dark noise is approximately 14 dB below the shot noise level. The corresponding SNR vs displacement is shown in Fig. 3(b). The two smooth real lines are theoretical results obtained using Eq. (8). Trace (c2) clearly increases faster than trace

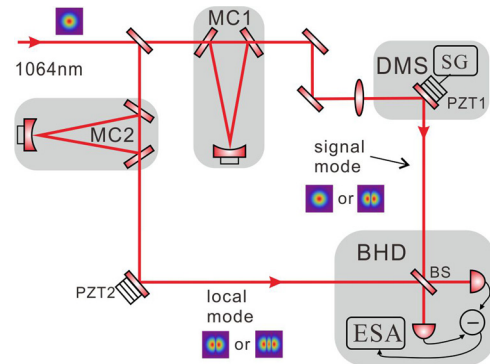


FIG. 2. Experimental setup. MC1, MC2: mode converters, DMS: displacement modulation system, PZT1, PZT2: piezoelectric transducers, SG: signal generator, BS: 50/50 beam splitter, BHD: balanced homodyne detection, ESA: electronic spectrum analyzer.

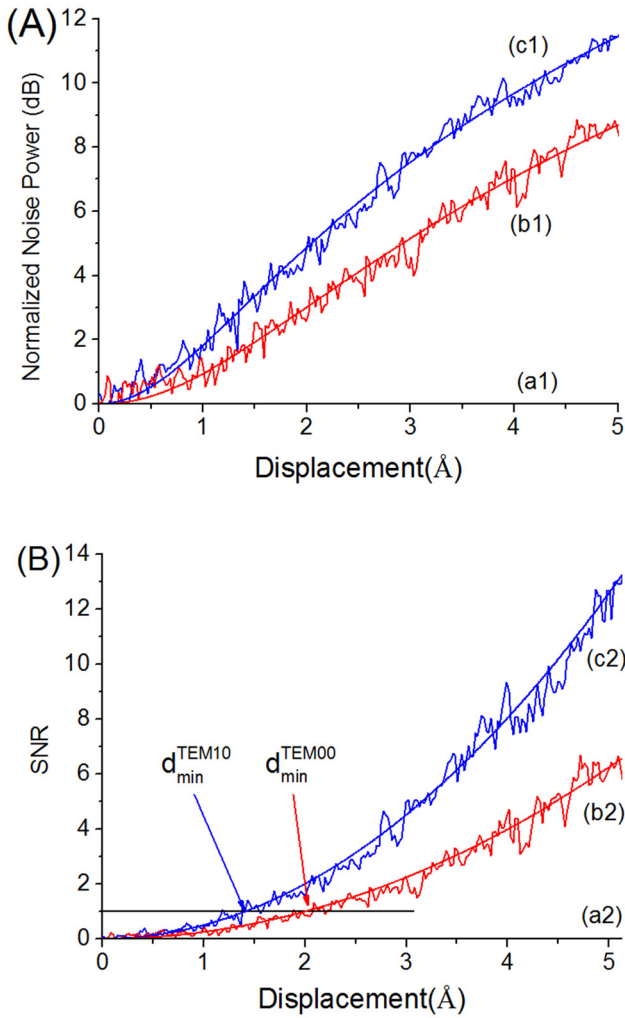


FIG. 3. (a) Normalized signal power measured in the ESA vs beam displacement: (a1) corresponds to the quantum noise, (b1) TEM_{00} signal mode, and (c1) TEM_{10} signal mode. (b) Signal-to-noise ratio plotted against displacement. Traces (a2), (b2), and (c2) correspond to traces (a1), (b1), and (c1), respectively.

(b2) as displacement increases, signifying that the measured SNR increases with increasing mode order under the same conditions (displacement, optical power, and fundamental mode beam waist). Consequently, measurement precision improved using high-order modes.

From Eq. (9), the minimum measurable displacements for the TEM_{00} mode and for TEM_{10} mode are, respectively,

$$d_{TEM00}^{int,BHD} = \frac{w_0}{2\sqrt{P_s \lambda / (hc \times RBW)}} = 2 \text{ \AA}, \quad (10)$$

$$d_{TEM10}^{int,BHD} = d_{TEM00}^{int,BHD} / \sqrt{2} = 1.4 \text{ \AA}, \quad (11)$$

where $\lambda = 1064 \text{ nm}$ is the wavelength, h is the Planck's constant, and c is the speed of light in vacuum.

With SNR of 1 in Fig. 3(b), we obtained a minimum measurable displacement of almost 1.4 \AA and 2 \AA for the TEM_{00} and TEM_{10} signal beam, respectively, and a

1.41 -factor improvement in measurement precision, in good agreement with theory.

In conclusion, we have theoretically presented a scheme for optical transverse-displacement measurements based on high-order Hermite-Gauss modes. Minimum measurable displacements attained the limit deduced from the QCR bound. With an intermediate local-oscillator mode, we also give preliminary experimental results of displacement measurements using coherent TEM_{00} and TEM_{10} as signal modes. The minimum measurable displacement using the TEM_{10} mode outperforms that for the TEM_{00} mode, in good agreement with theory. This scheme can be widely used in precision measurements, and, perhaps, even in gravitational wave detection and quantum measurements.

This research was supported by the National Basic Research Program of China (No. 2010CB923102), NSFC Project for Excellent Research Team (Grant No. 61121064), and the National Natural Science Foundation of China (Grant Nos. 11274212 and 11174189).

¹G. Meyer and N. M. Amer, *Appl. Phys. Lett.* **53**, 1045 (1988).

²C. A. J. Putman, B. G. De Groot, N. F. Van Hulst, and J. Greve, *J. Appl. Phys.* **72**, 6 (1992).

³R. M. Simmons, J. T. Finer, S. Chu, and J. A. Spudich, *Biophys. J.* **70**, 1813 (1996).

⁴F. Gittes and C. F. Schmidt, *Opt. Lett.* **23**, 7 (1998).

⁵D. G. Grier, *Nature* **424**, 810 (2003).

⁶M. Kolobov, *Rev. Mod. Phys.* **71**, 1539 (1999).

⁷V. Delaubert, N. Treps, C. Fabre, H.-A. Bachor, and P. Réfrégier, *Europhys. Lett.* **81**, 44001 (2008).

⁸L. Lugiato, A. Gatti, and E. Brambilla, *J. Opt. B: Quantum Semiclassical Opt.* **4**, S176 (2002).

⁹M. A. Taylor, J. Janousek, V. Daria, J. Knittel, B. Hage, H.-A. Bachor, and W. P. Bowen, *Nat. Photonics* **7**, 229 (2013).

¹⁰B. Willke, in *Proceedings of the IEEE Quantum Electronics and Laser Science Conference (QELS '05)*, Maryland, USA, 22-27 May, 2005, pp. 773-775.

¹¹N. Treps, N. Grosse, W. P. Bowen, C. Fabre, H.-A. Bachor, and P. K. Lam, *Science* **301**, 940 (2003).

¹²K. Wagner, J. Janousek, V. Delaubert, H. Zou, C. Harb, N. Treps, J. F. Morizur, P. K. Lam, and H. A. Bachor, *Science* **321**, 541 (2008).

¹³J. Gao, F. Cui, C. Xue, C. Xie, and P. Kunchi, *Opt. Lett.* **23**, 870 (1998).

¹⁴M. T. L. Hsu, V. Delaubert, P. K. Lam, and W. P. Bowen, *J. Opt. B: Quantum Semiclassical Opt.* **6**, 495 (2004).

¹⁵V. Delaubert, N. Treps, M. Lassen, C. C. Harb, C. Fabre, P. K. Lam, and H.-A. Bachor, *Phys. Rev. A* **74**, 053823 (2006).

¹⁶O. Hosten and P. Kwiat, *Science* **319**, 787 (2008).

¹⁷P. Dixon, D. Starling, A. Jordan, and J. Howell, *Phys. Rev. Lett.* **102**, 173601 (2009).

¹⁸L. Novotny, E. Sánchez, and X. S. Xie, *Ultramicroscopy* **71**, 21 (1998).

¹⁹J. Du, W. Li, R. Wen, G. Li, P. Zhang, and T. Zhang, *Appl. Phys. Lett.* **103**, 083117 (2013).

²⁰V. Delaubert, N. Treps, C. C. Harb, P. K. Lam, and H.-A. Bachor, *Opt. Lett.* **31**, 1537 (2006).

²¹V. Giovannetti, S. Lloyd, and L. Maccone, *Science* **306**, 1330 (2004).

²²O. Pinel, J. Fade, D. Braun, P. Jian, N. Treps, and C. Fabre, *Phys. Rev. A* **85**, 010101 (2012).

²³B. Willke, N. Uehara, E. K. Gustafson, R. L. Byer, P. J. King, S. U. Seel, and R. L. Savage, *Opt. Lett.* **23**, 1704 (1998).

²⁴M. Lassen, V. Delaubert, C. C. Harb, P. K. Lam, N. Treps, and H.-A. Bachor, *J. Eur. Opt. Soc. Rapid Publ.* **1**, 6003 (2006).